GA-BASED FEEDBACK CONTROL SYSTEM FOR DRAG REDUCTION IN TURBULENT CHANNEL FLOW

Yuji Suzuki, Takashi Yoshino, Tsuyoshi Yamagami and Nobuhide Kasagi

Department of Mechanical Engineering, The University of Tokyo,
Hongo 7-3-1, Bunkyo-ku, Tokyo, 113-8656, Japan.

ysuzuki@thtlab.t.u-tokyo.ac.jp

ABSTRACT

A prototype system for feedback control of wall turbulence is developed, and its performance is evaluated in a physical experiment. Arrayed micro hot-film sensors with a spanwise spacing of 1 mm are employed for the measurement of the streamwise shear stress fluctuations, while arrayed magnetic actuators having 3 mm in spanwise width are used to introduce control input through wall deformation. A digital signal processor having a time delay of 0.1 ms is employed to drive output voltage for the actuators. Feedback control experiments are made in a turbulent air channel flow. Noise-tolerant genetic algorithm is employed to optimize control parameters. It is found that the wall shear stress is decreased by up to 6 % in physical experiments for the first time. Reynolds shear stress close to the wall is decreased by the present control scheme. By using conditional sampling of DNS database, we found that the present control scheme effectively captures the near-wall shear layer, and introduces wall-normal velocity away from the wall underneath near-wall high-speed regions.

INTRODUCTION

Active control of wall turbulence was proposed a few decades ago (e.g., Wilkinson, 1990), and feedback control algorithm especially for drag reduction has been extensively pursued with the aid of direct numerical simulation (DNS) (Moin & Bewley, 1994; Gad-el-Hak, 1996; Kasagi, 1998). In order to realize such a control system, coherent structures such as the near-wall streamwise vortices, which are responsible for the regeneration cycle of turbulence and wall skin friction, should be detected by wall sensors, and selectively manipulated by the motion of actuators mounted on the wall. Although the coherent structures have generally very small spatio-temporal scales, recent development of microelectromechanical systems (MEMS) technology has made it possible to fabricate flow sensors and mechanical actuators of submillimeter scale (Udell et al., 1990; Ho & Tai, 1996). However, attempts to develop such a feedback control system in physical experiments are very few; Rathnasingham & Breuer(1997)

made a control system incorporating four hot-film shear stress sensors, a piezoelectric cantilever beam actuator, and a DSP controller. They reported reduction in turbulent intensities, but number of the devices is insufficient to observe substantial control effect in their system. Tsao et al.(1997) developed a sophisticated integrated chip consisting of hot-film shear stress sensors, magnetic flap actuators, and a drive circuit. However, since 22 masks were needed to develop such a complicated device, fabrication yield remained low and the control effect using arrays of their device was not made. Therefore, even in laboratory experiments, no drag reduction was achieved using feedback control systems in previous studies.

The objectives of the present study are to develop a prototype of feedback control system with arrayed micro hot-film shear stress sensors and wall-deformation magnetic actuators, and to evaluate its performance of drag reduction in a turbulent channel flow.

FEEDBACK CONTROL SYSTEM WITH GA-BASED ALGORITHMS

Figure 1a shows our prototype control system. It has four sensor rows and three actuators rows in between. Each sensor row has 48 micro wall-shear stress sensors with 1mm spacing, and each actuator row has 16 wall-deformation actuators with 3mm spacing. Magnified view and schematic of the cross section of the shear stress sensor is shown in Fig. 1b. A platinum hot-film is deposited on a SiN_X diaphragm ($400 \lozenge 400 \mu m^2$) of 1 μm in thickness, and a 200 μm-deep air cavity is formed underneath. We found that the frequency response of this first generation sensor is somewhat low, and the gain drops to 0.5 at $f > 170$ Hz (Yoshino et al., 2003). However, it is also found that the spanwise two-point correlation of τ'_w measured with the arrayed sensors is in good accordance with the DNS data. Therefore, the near-wall coherent structures, which are the target of the feedback control, can be well captured with the present wall shear stress sensors.

Endo et al.(2000) obtained 12 % drag reduction in their DNS

of a turbulent channel flow, in which arrayed wall shear stress sensors and wall-deformation actuators of finite spatial dimensions are assumed. They found that wall-deformation elongated in the streamwise direction is effective in attenuating near-wall vortices. Based on their results, miniature magnetic actuators are employed to introduce control input through wall deformation. As shown in Fig. 1c, a silicone rubber sheet of 0.1 mm in thickness is used as an elastic membrane, on which a 0.5 mm-thick rare-earth permanent magnet is glued. A miniature copper coil elongated in the streamwise direction are used to deform the membrane with magnetic force. Dimensions of the membrane are chosen as 2.4 mm (29 ν/u_τ) and 14 mm (168 ν/u_τ) respectively in the spanwise and streamwise directions. The resonant frequency is 800 Hz for 10 $Vp\text{-}p$ signal with a maximum amplitude of about 50 μm.

A digital signal processor (DSP) system (MPC7410, MTT Inc.) with 224 analog input and 96 output channels is used as the controller of the present system. The output voltage of the constant temperature circuits for the hot-film sensors are digitized with 14 bit AD converters. The control signals for the actuators are then computed with the DSP, and converted back to analog signals using 14 bit DA converters. The processing time of the DSP is within 0.1 ms, and the repetition frequency of the control loop is 5 kHz, which is believed to be sufficiently high if compared with the characteristic time scale of the turbulence.

A turbulent air channel flow facility is employed for the evaluation of the present feedback control system (Fig. 2a). The cross section of the channel is 50 ◊ 500 mm², and the test section is located 4 m downstream from the inlet, where the flow is fully-developed. The control system is placed at the bottom wall of the test section. The bulk mean velocity U_m is set to be 3 m/s, which corresponds to the Reynolds number Re_τ based on the wall friction velocity u_τ and the channel half-width of 300. Under the present flow condition, one viscous length and time unit correspond to 0.09 mm and 0.5 ms, respectively. Thus, the mean diameter of the near-wall streamwise vortices is estimated to be 2.7 mm, and its characteristic time scale is 7.5 ms. The flow field is measured with a three-beam two-component LDV system (DANTEC, 60X51) as shown in Fig. 2b. The measurement volume is about ϕ160 μm x 3.5 mm.

It is well known that the control scheme based on the spanwise component of the wall shear stress fluctuation is effective in drag reduction (e.g., Lee et al., 1998). However, Yoshino et al. (2001) found that its accurate measurement is found to be extremly difficut even if MEMS sensor is employed, because instantaneous spanwise distribution of the steamwise velocity deteriorates the spanwise component measured with multiple-element hot-film sensors (Suzuki & Kasagi, 1992). Suzuki et al. (2001) employ the streamwise wall shear stress fluctuations as the sensor information, and apply local wall blowing/suction determined with a linear combination of the wall shear stress fluctuations at three locations aligned in the spanwise direction. They optimize the control parameters using genetic algorithms (GA), and obtain 10 % drag reduction in their DNS. This result encourage us to develop a GA-based feedback control system using the streamwise wall shear stress. Driving voltage of each wall-deformation actuator E_A is determined with a linear combination of the streamwise wall shear stress fluctuations $\tau_w{'}_i$, i.e.,

$$E_A = \sum_{i=1,3} W_i \tau'_{w,i} \tag{1}$$

where $\tau_w{'}_i$ is measured with three sensors located upstream as shown in Fig. 3. The spacing between neighboring sensor used in the present control scheme is 1 mm (36 ν/u_τ). The center of the actuator is located about 100 viscous units downstream of the sensors. Note that actuators move upwards when E_A is positive, while downwards when negative.

The control variables W_i are optimized in such a way that the mean wall shear stress measured with three sensors at the most downstream location is minimized. The cost function J, which equals the drag reduction rate, is then defined by

$$J = 1 - \frac{\sum_{j=1,3}\left(\int_0^T \tau_{w,j} dt\right)}{\sum_{j=1,3}\left(\int_0^T \tau_{w,j}|_{no-control} dt\right)}, \tag{2}$$

and J is maximized. Each W_i is expressed with a binary-coded string with 5 bits, which corresponds to a gene, and N individuals including a set of genes are made. Feedback control experiment using each individual, i.e., different set of W_is is independently carried out, and the cost function is calculated on line. Then, individuals having larger cost are statistically selected as parents, and offsprings are made through crossover operation. Finally, mutation at a given rate is applied to all genes of the N individuals. Probabilities of crossover and mutation are respectively chosen as 0.4 and 0.01. Elite selection strategy is also adopted, so that gene having maximum cost is always preserved. New generations are successively produced by repeating this procedure. The integration time $\forall T$ is chosen as 20 s ($\forall T^+$=4000), which is much longer than the characteristic time scale of the large scale motion. The population size N and number of generation are respectively chosen as 10 and 100. Thus, in total, 1000 trials with different set of control variables are made out of 2^{15}=32768 possible combination of genes.

We found in our preliminary experiment that the cost function J integrated over $\forall T$ has a bias error of -2%. It is conjectured that the bias error is due to the thermal cross-talk between sensors and actuators. Moreover, J also has relatively-large random error of about 3%. The random error is mainly due to the small temporal variation of air temperature, which is inevitable in the present experiment lasting for more than ten hours. Since the random error makes the genes stacked at local maxima or spurious optimum points, we employed a noise-tolerant GA method proposed by Tobita et al. (1998); in the present study, 7 out of total 10 genes are determined with the procedure described above, and the rest 3 genes are re-initialized with random numbers at each generation .

CONTROL EXPERIMENTS IN TURBULENT CHANNEL FLOW

Figure 4a shows the evolution of the cost function. The data are scattered in a wide range because of the genes with random number introduced. As the generation proceeds, more genes provides large positive J corresponding to drag reduction, and J reaches the maximum value of 0.11 at the 52th generation. If we consider the bias and random error in J mentioned above, it is reasonable to conclude that we have obtained 6±3% drag reduc-

tion. Figure 4b shows the distribution of the best W_i obtained, which corresponds to the optimum gene. It is found that W_is are all negative. Figure 4c shows probability density of J. Each gene is grouped into three categories depending on the sign of W_2 in Eq. (1). It is found that half of the genes tested in the GA-based trial have a similar trend as the best gene. For genes with large negative W_2, the distribution spreads widely and there exists a broad peak from 0.03 to 0.08. On the other hand, for genes with large positive or near-zero W_2, the distribution has a sharp peak at 0.02 corresponding to the bias error of the present experiment. Therefore, it is clear that drag reduction is achieved with negative W_is in the present experiment. Note that, when all W_is is kept positive without using the GA algorithms, no drag reduction is obtained (not shown).

Figure 5 shows turbulent statistics above an actuator measured with LDV. In this paticular measurement, only a single actuator is moving according to the feedback scheme with the optimum gene. The wall friction velocity and the wall elevation of the first measurement station are estimated by fitting the near-wall mean velocity profile to a mixing length model (McEligot, 1984). Experimental data for the unmanipulated flow are in good agreement with the DNS data (Iwamoto et al., 2002). When the present feedback control is applied, the mean velocity profile and the rms values are unchanged. On the other hand, the Reynolds shear stress close to the wall is decreased as shown in Fig. 5c.

Figure 6 shows the near-wall Reynolds stress profile normalized with that for the unmanipulated case. By using a curve fitting of the present data, the drag reduction rate is computed with the FIK identity (Fukagata et al., 2002), which describes the contribution of the Reynolds stress to the wall skin friction in a fully-developed flow. The drag reduction rate thus estimated is found to be 0.6%, which is much smaller than the change in the wall shear stress. Nevertheless, the drag reduction is qualitatively confirmed through the present LDV measurement.

IMPLICATION OF THE PRESENT CONTROL SCHEME

Since optimum W_is are negative, actuators move downward when τ_w' is positive. However, it is not straightforward to interpret the effect of the present control scheme on the near-wall coherent structures. Thus, we made a conditional average of a DNS database (Iwamoto et al., 2002) in order to examine the flow structure near the actuators. Since the wall deformation is much smaller than the thickness of the viscous sublayer, the deformed shape itself has little effect on the flow field. Instead, the wall-normal flow velocity induced by the wall motion can modify the flow field (Endo et al., 2000). Therefore, we define q as the indicator of the wall velocity using the time derivative of E_A,

$$q \int \frac{dE_A}{dt} = \frac{d}{dt}\left(\sum_{i=1,3} W_i \tau_{w,i}' \right). \tag{3}$$

Strictly speaking, the wall velocity is not proportional to q due to the nonlinear response of the actuator, but we believe that conditionally-averaged field based on large q should be associated with large wall velocity.

Figure 7a shows a 3-D structure associated with $q > q_{rms}$ corresponding to the upward motion of the wall. Low- and high-speed regions are respectively observed upstream and downstream the detection point. Figure 7b shows the x-y plane including the detection point. Internal shear layer having a small tilt angle to-ward the wall is clearly seen. This is because, positive q also corresponds to negative $d\tau_w/dt$, corresponding to the deceleration at the detection point. Figure 7c shows velocity vectors and contours of the streamwise velocity fluctuations in a cross-stream plane located at 100 viscous units downstream the detection point, where the center of the actuator is located. It is found that a high-speed region is located near the wall, and the wall-normal velocity near the buffer layer is negative. There, when $q > q_{rms}$, the present control scheme detects the internal shear layer, and induces upward wall velocity underneath the near-wall high-speed regions.

Although it is not shown here, the conditional sampling for $q < -q_{rms}$ is also made, which corresponds to acceleration at the detection point and to the downward motion of the wall. It is found that the conditional-averaged structure is somewhat smeared out, and the wall-normal velocity near the buffer layer is slightly negative, which is in-phase with the motion of the actuator. Further analysis is necessary for more detailed control mechanism.

CONCLUSIONS

The prototype of the feedback control system for wall turbulence is developed using arrayed micro hot-film sensors and arrayed magnetic wall-deformation actuators. Driving voltage of the actuators is assumed to be a linear combination of the wall shear stress fluctuations measured at three locations upstream, and the weights are optimized by using a noise-tolerant genetic algorithm in such a way that the time integral of the wall shear stress is minimized. We have obtained about 6 % skin friction reduction in a turbulent channel flow for the first time. The Reynolds shear stress is found to be decreased near the wall. We also found in conditional sampling of a DNS database that, with the present control scheme, the wall-deformation actuators move upwards beneath the near-wall high-speed regions.

REFERENCES
Choi, H., Moin, P., and Kim, J., 1994, "Active Turbulence Control for Drag Reduction in Wall-Bounded Flows," J. Fluid Mech., Vol. 262, pp. 75-110.
Endo, T., Kasagi, N., and Suzuki, Y., 2000, "Feedback Control of Wall Turbulence with Wall Deformation," Int. J. Heat & Fluid Flow, Vol. 21, pp. 568-575.
Fukagata, K., Iwamoto, K., and Kasagi, N., 2002, "Contribution of Reynolds Stress Distribution to the Skin Friction in Wall-Bounded Flows," Phys. Fluids, Vol. 14, pp. L73-L76.
Gad-el-hak, M., 1996, "Modern Developments in Flow Control," Appl. Mech. Rev., Vol. 49, pp. 365-379.
Ho, C.-M., and Tai, Y.-C., 1996, "Review: MEMS and its Applications for Flow Control," ASME J. Fluids Eng. Vol. 118, pp. 437-447.
Iwamoto, K., Suzuki, Y., and Kasagi, N., 2002, "Reynolds Number Effect on Wall Turbulence: Toward Effective Feedback Control," Int. J. Heat & Fluid Flow, Vol. 23, pp. 678-689.
Kasagi, N., 1998, "Progress in Direct Numerical Simulation of

Turbulent Transport and Its Control," Int. J. Heat & Fluid Flow, Vol. 19, pp. 128-134.

Lee, C., Kim, J., and Choi, H., 1998, "Suboptimal Control of Turbulent Channel Flow for Drag Reduction," J. Fluid Mech., Vol. 358, pp. 245-258.

McEligot, D. M., 1984, "Measurement of Wall Shear Stress in Accelerating Turbulent Flows," Max-Planck-Institute für Strömungsforschung, Göttingen.

Moin, P., and Bewley, T., 1994, "Feedback Control of Turbulence," Appl. Mech. Rev., Vol. 47, pp. S3-S13.

Rathnasingham, R., and Breuer, K., 1997, "System Identification and Control of a Turbulent Boundary Layer," Phys. Fluids, Vol. 9, pp. L1867-L1869.

Suzuki, Y., and Kasagi, N., 1992, "Evaluation of Hot-Wire Measurements in Wall Shear Turbulence Using a Direct Numerical Simulation Database," Exp. Therm. Fluid Sci., Vol. 5, pp. 69-77.

Suzuki, Y., Morimoto, S., Iwamoto, K., and Kasagi, N., 2001, "Feedback control of wall turbulence based on the streamwise wall shear stress," Bull. Am. Phys. Soc., Vol. 46, p. 185.

Tobita, T., Fujino, A., Segawa, K., Yoneda, K., and Ichikawa, Y., 1998, "A parameter tuning method for an elevator group control system using a genetic algorithm," Electrical Engineering in Japan, Vol. 124, pp. 55-64.

Tsao, T., Jiang, F., Miller, R. A., Tai, Y.-C., Gupta, B., Goodman, R., Tung, S., and Ho, C. -M., 1997, "An Integrated MEMS System for Turbulent Boundary Layer Control," Tech. Digest Int. Conf. on Solid-State Sensors and Actuators (Transducers '97), Chicago, pp. 315-317.

Udell, K. S., Pisano, A. P., Howe, R. T., MUller, R. S., and White, R. M., 1990, "Microsensors for Heat Transfer and Fluid Flow Measurements," Exp. Therm. Fluid Sci., Vol. 3, pp. 52-59.

Wilkinson, S. P., 1990, "Interactive Wall Turbulence Control," in Prog. Astronautics and Aeronautics: Viscous Drag Reduction in Boundary Layers, Bushnell, D. M., and Hefner, J. N., eds., Vol. 123, (1990), pp. 479-509, AIAA.

Yoshino, T., Suzuki, Y., Kasagi, N., and Kamiunten, S., 2001, "Assessment of the Wall Shear Stress Measurement with Arrayed Micro Hot-film Sensors in a Turbulent Channel Flow, " Proc. 2nd Int. Symp. Turbulence and Shear Flow Phenomena, Stockholm, Vol. II, pp. 17-22.

Yoshino, T., Suzuki, Y., Kasagi, N., and Kamiunten, S., 2003, "Optimum Design of Micro Thermal Flow Sensor and Its Evaluation in Wall Shear Stress Measurement," Proc. IEEE Int. Conf. MEMS 2003, Kyoto, pp. 193-196.
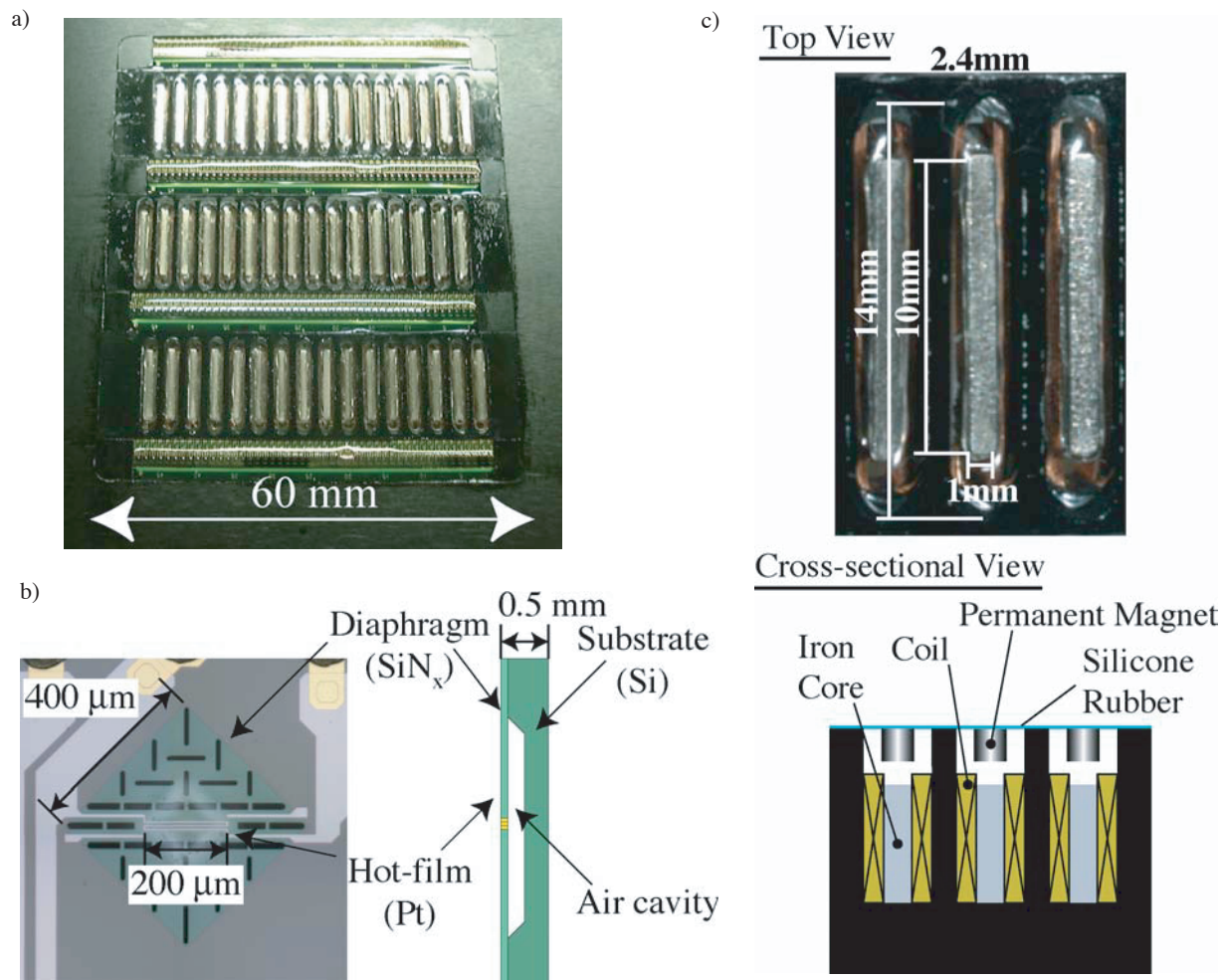
Figure 1 Prototype feedback control system for wall turbulence. a)Plane view of the system having 192 wall shear stress sensors and 48 wall-deformation actuators, b)Magnified view of a sensor, c)Magnified view of actuators.
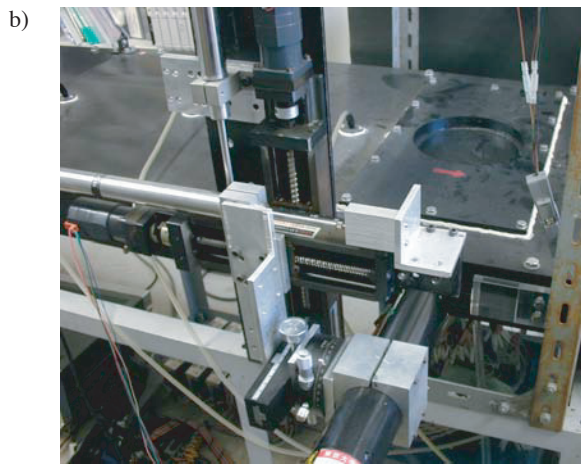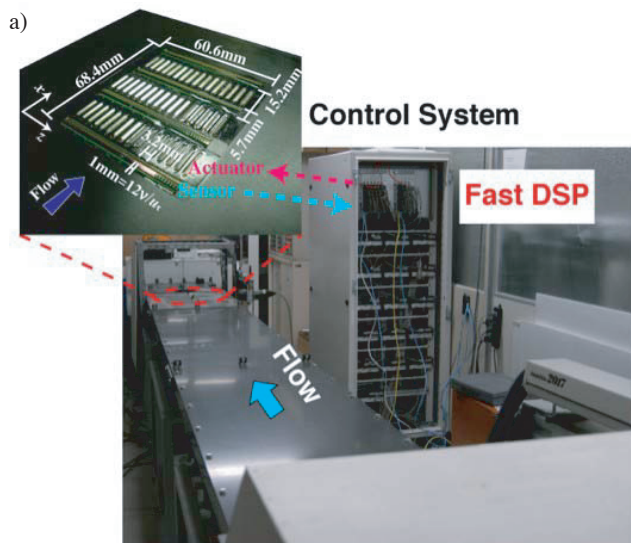
Figure 2 Experimental setup. a)Turbulent air channel flow facility and DSP control system, b)Test section and LDV traversing mechanism.
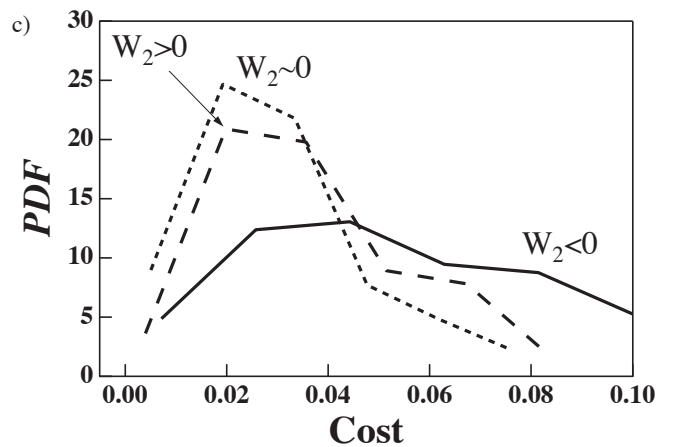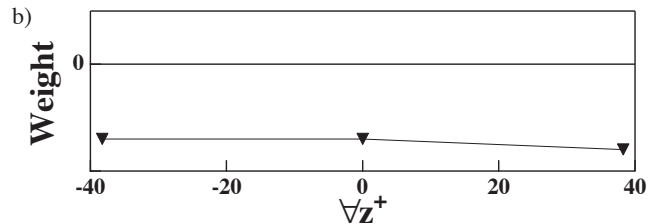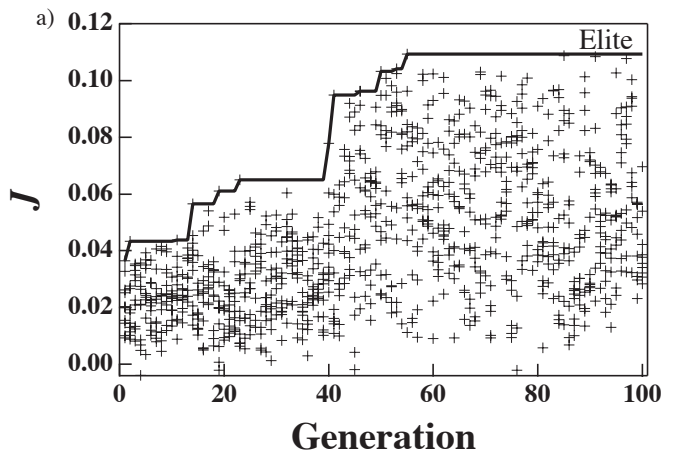
Figure 4 Result of GA-based feedback control in a turbulent channel flow. a)Cost function versus generation, b)Optimum weight, c)Probability density of J depending on the sign of W_2.

$$J = 1 - \frac{\sum_{j=1,3}\left(\int_0^T \tau_{w,j}\,dt\right)}{\sum_{j=1,3}\left(\int_0^T \tau_{w,j}\big|_{no\ control}\,dt\right)}$$

$$T = 20s = 4 \Diamond 10^4 \nu / u_\tau^2$$

$$E_A = C \sum_{i=1}^{3} W_i\left(\tau_i - \overline{\tau_i}\right)$$

W_i : Optimized by GA
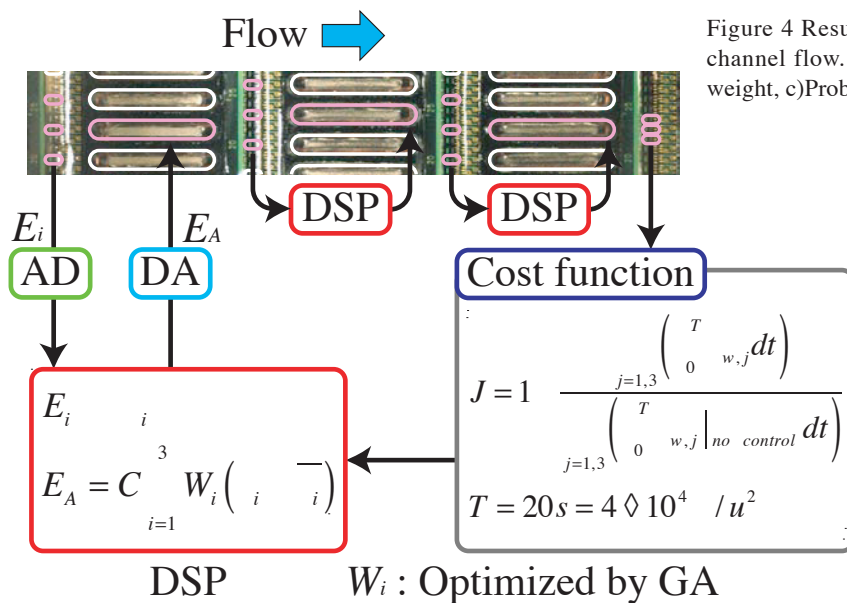
Figure 3 Schematic of the GA-based feedback control system and arrangement of shear stress sensors and actuators in a control unit.
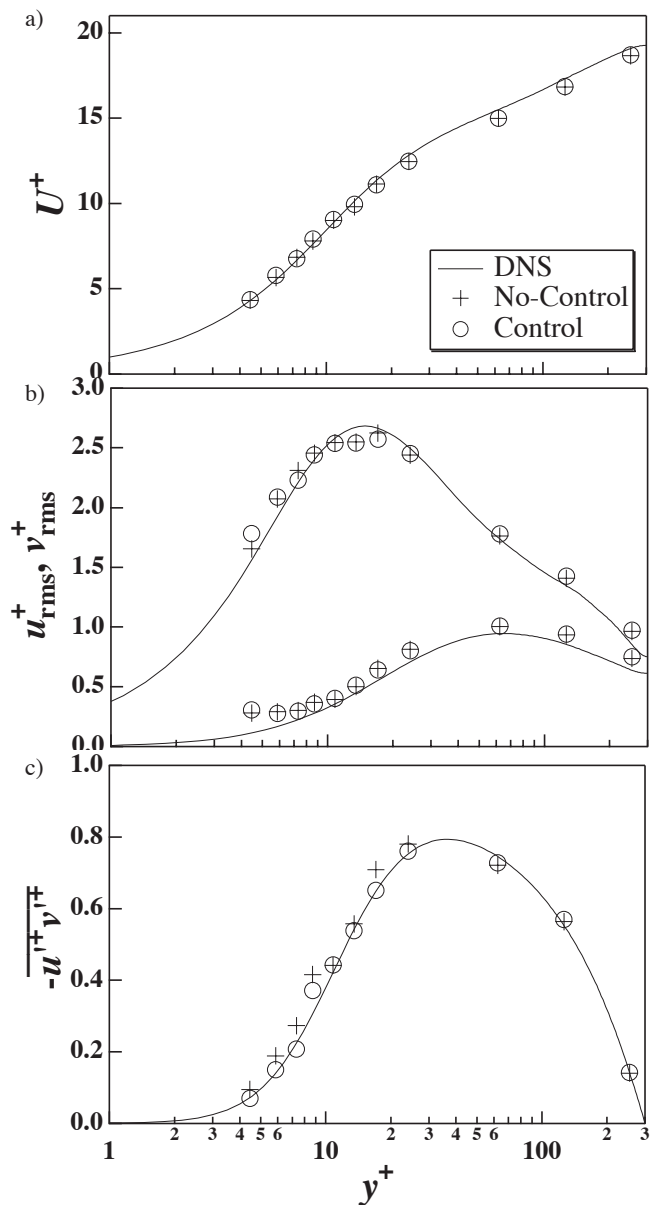
Figure 5 Turbulent statistics above the center of an actuator measured with LDV. a)Mean velocity profile, b)RMS values of turbulent fluctuations, c)Reynolds shear stress. The wall friction velocity is estimated for unmanipulated flow.

$$f(y^+) = 0.98 - 0.79 \exp(- 0.24\, y^+)$$
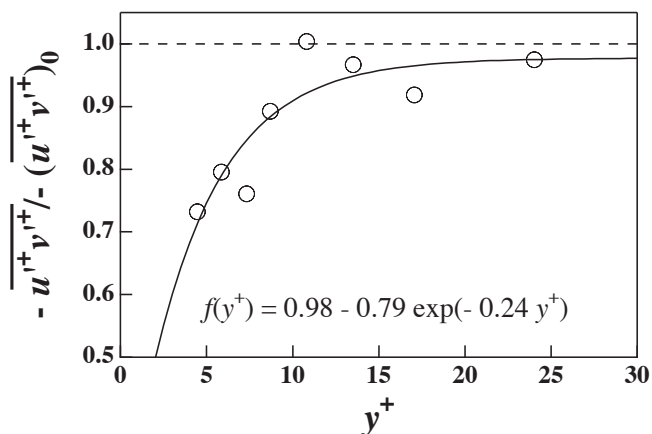
Figure 6 Normalized Reynolds stress profile close to the wall.
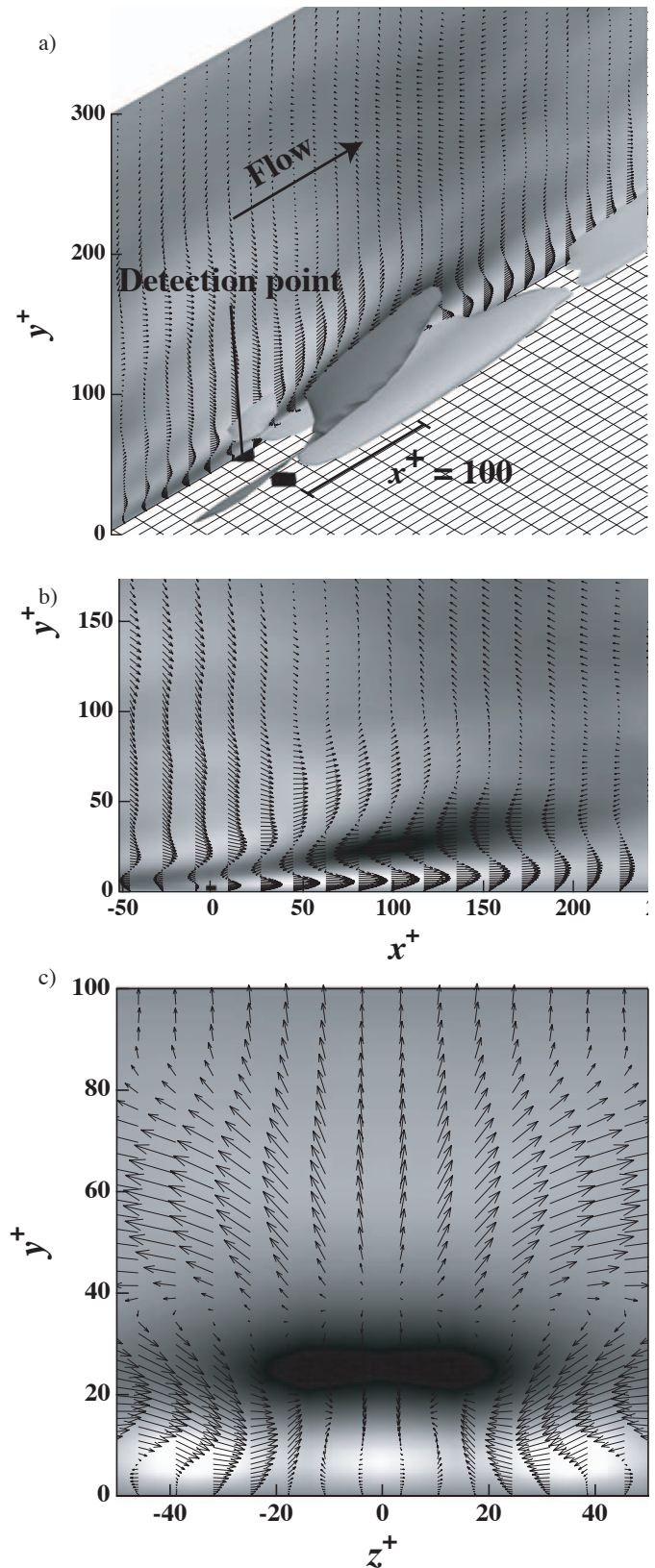
Figure 7 Conditional-averaged velocity field associated with events $q > q_{rms}$. a)Bird's eye view, b) Contours in the x-y plane, c) Contours and the cross-stream vectors in the y-z plane at $x^+=100$. Black to white, $<u^+> = -0.5$ to 0.5. DNS database of an unmanipulated channel flow at $Re_\tau=300$ is employed in order to extract the flow structures.